Tomographic analysis with the weak lensing convergence one-point statistics

Lina Castiblanco

Cora Uhlemann

Joachim Harnois-Deraps

Alexandre Barthelemy

Newcastle University

Theoretical Modeling of Large-Scale Structure of the Universe 2024


https://www.desi.lbl.gov/

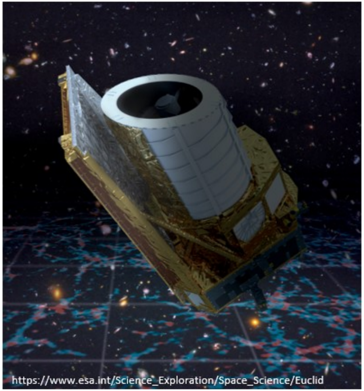
https://www.esa.int/Science_Exploration/Space_Science/Euclid


https://gallery.lsst.org/bp/#/

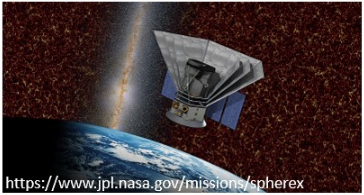
https://www.jpl.nasa.gov/missions/spherex


https://www.physics.ox.ac.uk/research/group/square-kilometre-array-ska


https://www.sdss3.org/


We are in the era of
precision cosmology
https://mapoftheuniverse.net/

The large-scale structure of the universe, LSS

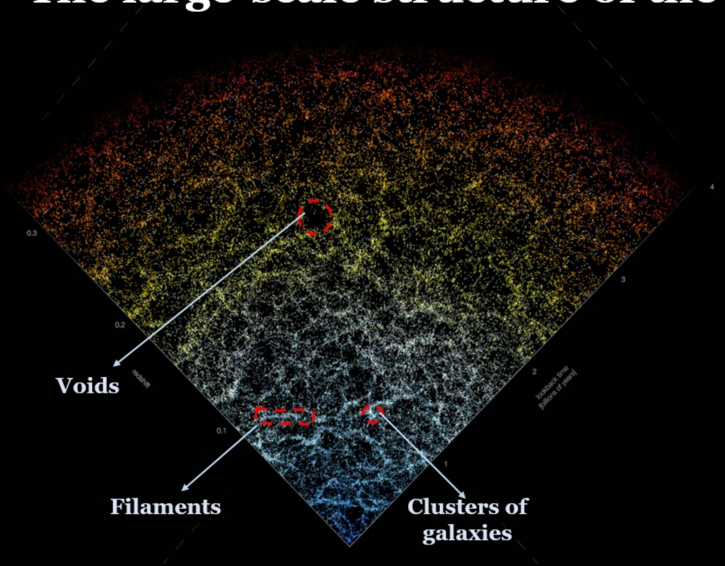

Imagen credit: https://mapoftheuniverse.net/

The large-scale structure of the universe, LSS

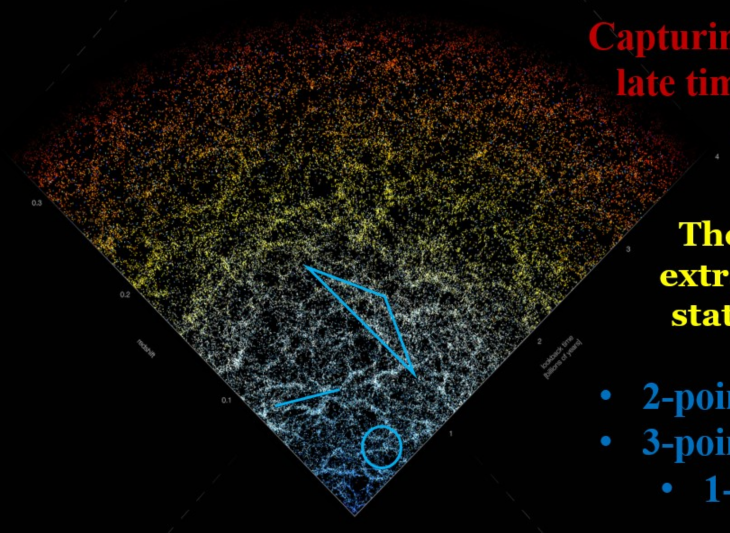

Capturing the non-Gaussian late time information is a challenge.

The information is extracted by using the statistics of the LSS.

- **2-point correlations**
- **3-point correlations**
- **1-point PDF**

Imagen credit: https://mapoftheuniverse.net/

One-Point PDF

Encodes information about the non-Gaussian late-time density field

Powerful tool that allows extracting the cosmological information

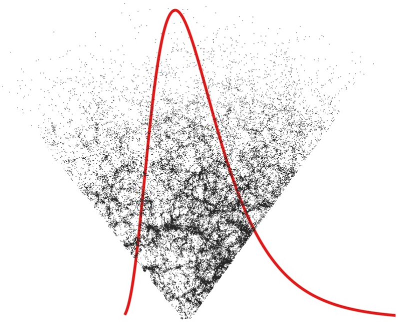

Straightforward to measure from simulated and observed data

Theoretically predicted with accuracy on mildly nonlinear scales.

Galaxy clustering N_g

C.Uhlemann, O.Friedrich, F.Villaescusa-Navarro, A.Banerjee, S.Codis (2019)

Weak lensing κ

A.Boyle, C.Uhlemann, O.Friedrich, A.Barthelemy, S.Codis, F.Bernardeau, C.Giocoli, M.Baldi (2021)

Covariance Modelling

C.Uhlemann, O.Friedrich, A.Boyle, A.Gough, A.Barthelemy (2022)

Measuring the one-point PDF

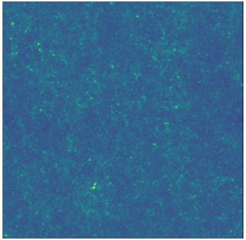

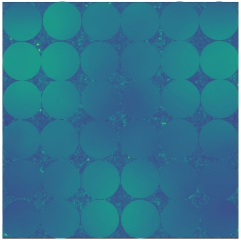

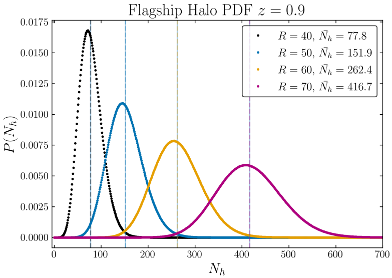

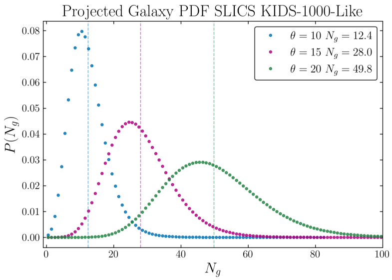

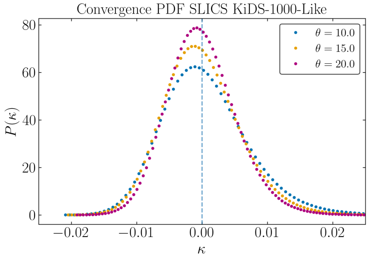

- Divide the distribution into various volumes
- Overlaping cells are allowed
- Smooth the field on each cell
- Count objects in each cell
- Plot a histogram

Gravitational weak lensing

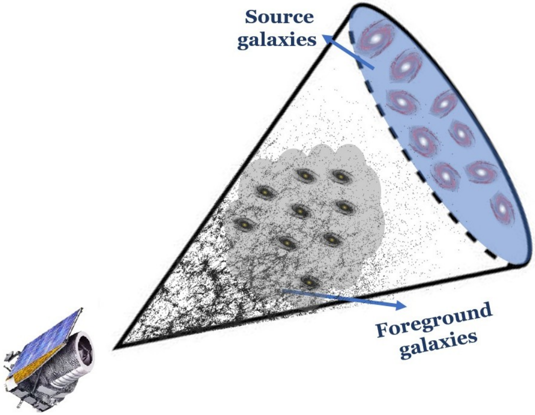

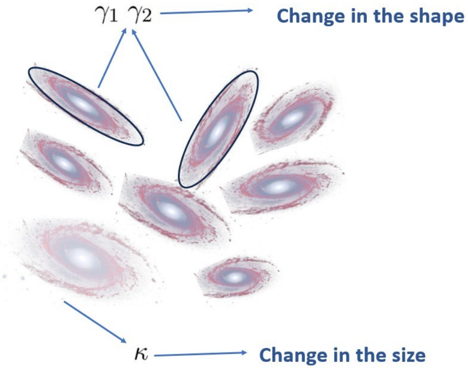

$$|\gamma_1| \ll 1 \qquad |\gamma_2| \ll 1 \qquad |\kappa| \ll 1$$

PDF modelling for projected fields

$$\kappa(\boldsymbol{\theta}) = \int_0^{R_s} dR\, w(R(z))\delta(R(z), R(z)\boldsymbol{\theta})$$

$$w(R) = \frac{3\Omega_m H_0^2}{2c^2} \int_0^{z_s} dz_s' \frac{[R(z_s') - R(z)]\, R(z)}{R(z_s')}(1+z)n(z_s')$$

Encodes the cosmological information

Cylindrical collapse

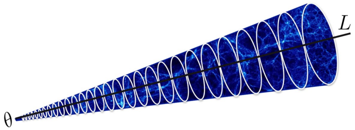

Large deviation theory

$$P^{ini}(\delta_L) = \sqrt{\frac{1}{2\pi\sigma_L^2}} \exp\left[-\frac{\delta_L^2}{2\sigma_L^2}\right]$$

Cumulants of the projected fields are given by the cumulants of the 3d matter density averaged over cylinders

$$\phi(i\lambda, R(z_s)) = \sum_{l=1}^{\infty} \frac{\lambda^l}{l!} \int_0^{R_s} dR\, w(R)^l \, \langle \delta_{\rm cyl}^l \rangle_c \, L^{l-1}$$

$$P(\kappa, z_s) = \int_{-\infty}^{\infty} \frac{d\lambda}{2\pi} e^{-i\lambda\kappa + \phi(i\lambda, z_s)}$$

CosMomentum Code

https://github.com/OliverFHD/CosMomentum

L2DT Code

https://github.com/AlexandreBarthelemy/L2DT-Lensing-with-Large-Deviation-Theory

Weak lensing κ PDF

- κ PDF Contains vast information around the peak.
- Including the shape noise effect is easy.

$$\sigma_{SN}^2 = \frac{\sigma_\epsilon^2}{n_g \Omega_\theta}$$

- Combining different scales enhances the constraining power of the PDF.
- The $P(\kappa)$ outperforms the information obtained from the two-point correlation functions.

A.Boyle, C.Uhlemann, O.Friedrich, A.Barthelemy, S.Codis, F.Bernardeau, C.Giocoli, M.Baldi (2021)

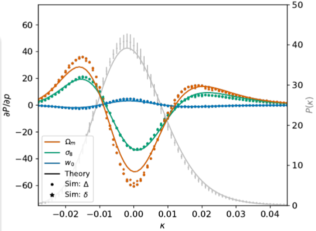

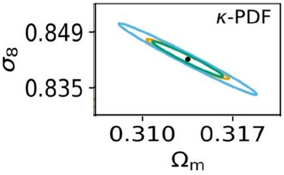

Euclid: HOWLS_KP (2023)

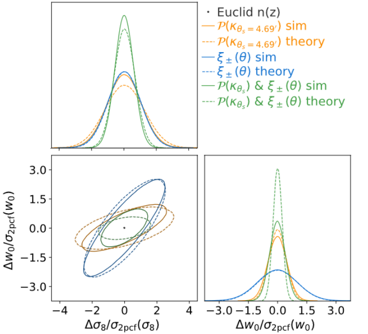

Overview of the Euclid mission (2024)

Unleashing cosmic shear information with the tomographic weak lensing PDF

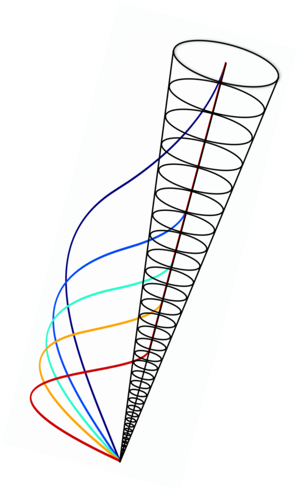

The source galaxies are distributed across various redshift bins.

Each redshift bin contains different cosmological information.

Enhance the precision of the constraints.

Break degeneracies.

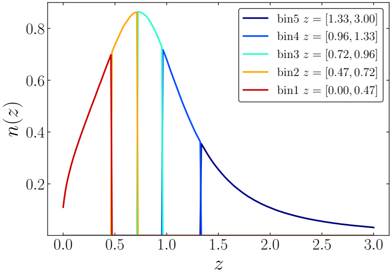

https://arxiv.org/pdf/2405.09651

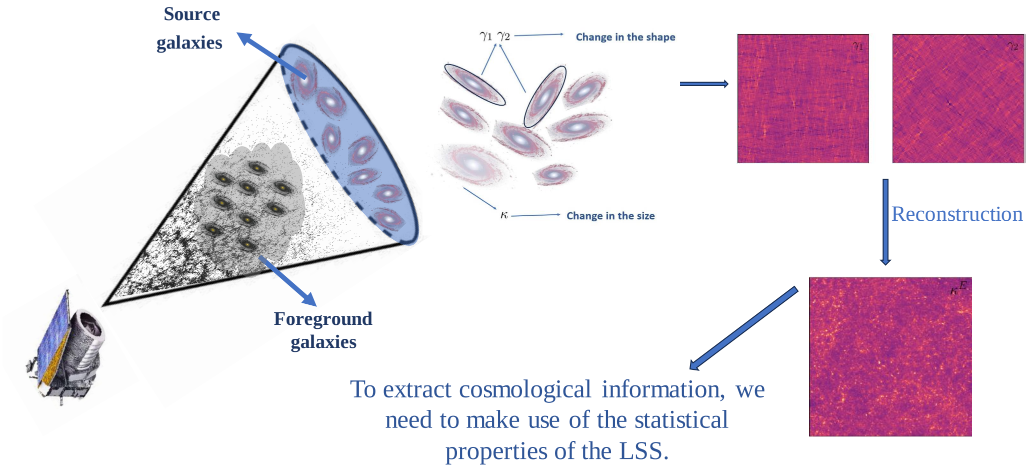
Source
galaxies
Foreground
galaxies
γ1 γ2
Change in the shape
κ
Change in the size
Reconstruction
To extract cosmological information, we
need to make use of the statistical
properties of the LSS.

Tomographic analysis with the κ PDF

The Scinet LightCone Simulations SLICS, Harnois-Deraps.et.al

Kaiser-Squires reconstruction of the κ field

$$\gamma = \gamma_1 + i\gamma_2 \Longrightarrow \kappa = \kappa_E + i\kappa_B$$

$$\hat{\kappa} = \hat{P}^* \hat{\gamma}, \qquad \hat{P} = \frac{k_1^2 - k_2^2 + 2ik_1k_2}{k_1^2 + k_2^2}$$

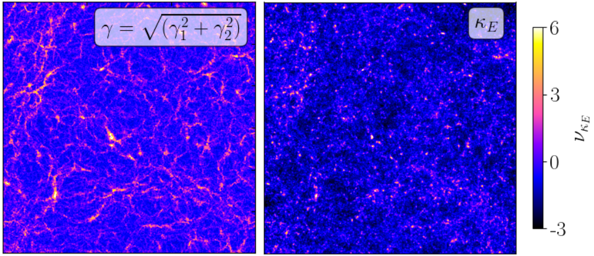

KS-Modeling: Rescaling of the non-linear variance

- The Non-linear power spectrum is modulated by the mixing matrix $M_{\ell\ell}^{EE,EE}$
- We rescale the Non-linear variance according with the modulation.

A.Barthelemy, A.Halder, Z.Gong, C.Uhlemann, (2023)

Tomographic analysis with the κ PDF

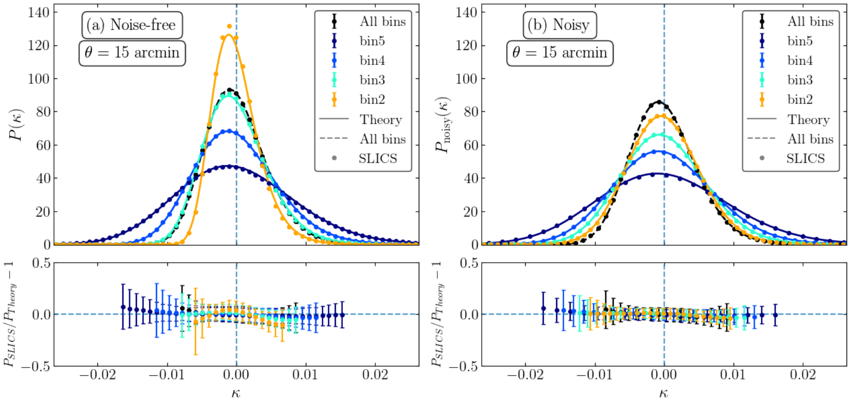

The theoretical predictions are accurate by less than 5%-level around the PDF peak.

Tomographic analysis with the κ PDF

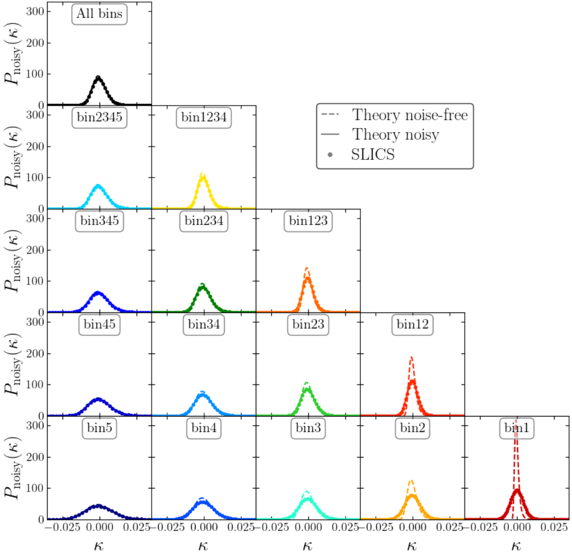

To minimise the impact of shape noise we consider combinations of consecutive redshift bins into (quarters, triples, pairs).

Tomographic analysis with the κ PDF

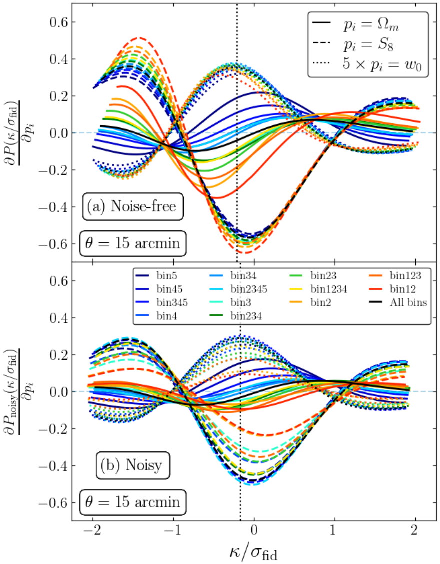

Changes in $S_8 = \sigma_8 \left(\frac{\Omega_{\rm m}}{0.3}\right)^{0.5}$ and w_0 mainly impact the variance.

Changes in $\Omega_{\rm m}$ may impact the skewness.

The variance is proportional to the square of the linear growth which depend on Ω_m and w_0.

$$S_3^{2D}(R_\theta) = \frac{\langle \delta^3(R_\theta)\rangle_c}{\langle \delta^2(R_\theta)\rangle_c^2} \approx \frac{36}{7} + \frac{3}{2}\frac{d\log \sigma_{\rm L}^2(R_\theta)}{d\log R_\theta}$$

Changes in $\Omega_{\rm m}$ change the reduced skewness due to the scale dependent variation of the variance.

Tomographic analysis with the κ PDF (Preliminary results)

Fisher analysis

$$F_{ij} = \frac{\partial P(\kappa)}{\partial p_i} C^{-1} \frac{\partial P(\kappa)}{\partial p_j}$$

The enhancement on the constraints with tomography is due to the additional information provided for the skewness at different redshift bins.

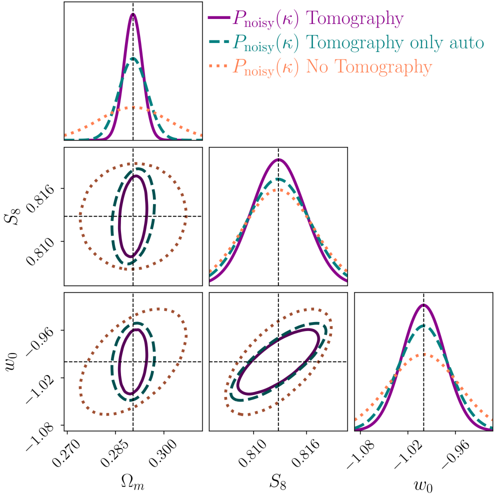

Tomographic analysis with the κ PDF (Preliminary results)

Fisher analysis

$$F_{ij} = \frac{\partial \boldsymbol{D}}{\partial p_i} \boldsymbol{C}^{-1} \frac{\partial \boldsymbol{D}}{\partial p_j}$$

$$\boldsymbol{D} = \left[P(\kappa), \xi^{+}(\gamma), \xi^{-}(\gamma) \right]$$

γ − 2PC

$$\xi^{\pm}(\theta) = \langle \gamma\gamma^{*} \rangle = \langle \gamma_1\gamma_1 \rangle \pm \langle \gamma_2\gamma_2 \rangle$$

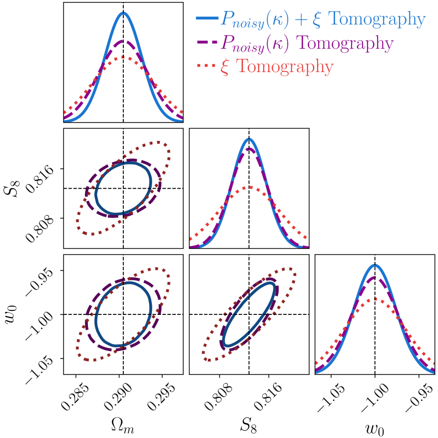

The $P(\kappa)$ outperforms the γ−2PCF due to the non-Gaussian information encoded in the skewness and higher order moments within the $P(\kappa)$.

Including Intrinsic Alignments (IA)

Intrinsic alignment arises from external gravitational tidal fields that generate physical correlations between the shapes of galaxies.

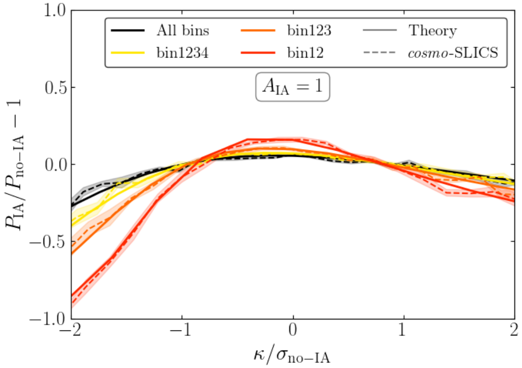

Non-linear alignment model

$$\delta_{\rm IA}(\chi\boldsymbol{\theta}, \chi) = -A_{\rm IA}\left(\frac{1+z}{1+z_0}\right)^{\alpha_{\rm IA}} \frac{\bar{C}\bar{\rho}(z)}{D(z)}\delta(\chi\boldsymbol{\theta}, \chi)$$

$$\kappa_{\rm IA}(\chi\boldsymbol{\theta}, \chi) = \int_0^{\infty} dz \frac{d\chi}{dz}\, n(z)\delta_{\rm IA}\left(\chi\boldsymbol{\theta}, \chi\right)$$

The impact of IA on the PDF modelling is included by modifying the projection kernel

$$w(\chi) \rightarrow w(\chi) + A(z)n(z)$$

Conclusions

- The tomographic $P(\kappa)$ can track the growth of structure and capture non-Gaussian information across different scales.
- The tomographic $P(\kappa)$ shows strong potential in constraining cosmological parameters.

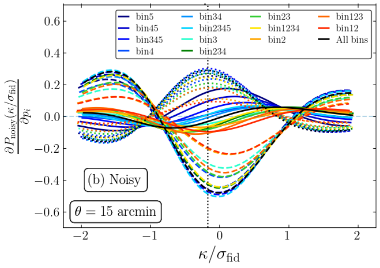

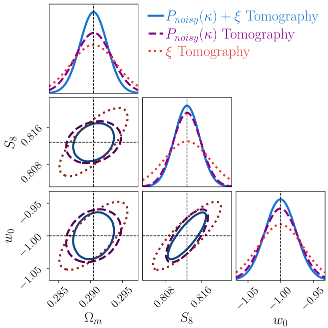

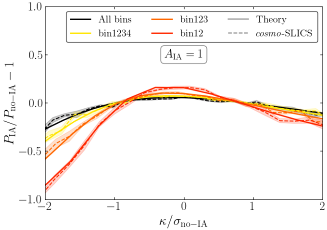

The theoretical model for the tomographic $P(\kappa)$ can be adapted to include weak lensing systematics.